Research Article

Journal of Geophysical Research: Oceans
DOI 10.1002/2017JC013264

Vulnerability of coral reefs to bioerosion from land-based sources of pollution

Nancy G.Prouty[1*] Anne Cohen[2], Kimberly K. Yates[3], Curt D. Storlazzi[1], Peter W. Swarzenski[1,4], and Darla White[5]

[1]U.S. Geological Survey, Coastal and Marine Geology, Pacific Coastal and Marine Science Center, Santa Cruz, CA 95060

nprouty@usgs.gov tel: +1-831-460-7526 fax: +1-831-427-4748

[2] Woods Hole Oceanographic Institution, Department of Geology and Geophysics, Woods Hole, MA 02543

[3 1]U.S. Geological Survey, St. Petersburg Coastal and Marine Science Center, 600 4th Street South, St. Petersburg, FL 33701

[4] International Atomic Energy Agency, 4, Quai Antoine 1er, 98000 Monaco, Principality of Monaco

[5] Division of Aquatic Resources, Department of Land and Natural Resources, Maui, HI 96793

*Corresponding author

Ocean acidification (OA), the gradual decline in ocean pH and [CO_3^{2-}] caused by rising levels of atmospheric CO_2, poses a significant threat to coral reef ecosystems, depressing rates of calcium carbonate ($CaCO_3$) production, and enhancing rates of bioerosion and dissolution. As ocean pH and [CO_3^{2-}] decline globally, there is increasing emphasis on managing local stressors that can exacerbate the vulnerability of coral reefs to the effects of OA. We show that sustained, nutrient rich, lower pH submarine groundwater discharging onto nearshore coral reefs off west Maui lowers the pH of seawater and exposes corals to nitrate concentrations 50 times higher than ambient. Rates of coral calcification are substantially decreased, and rates of bioerosion are orders of magnitude higher than those observed in coral cores collected in the Pacific under equivalent low pH conditions but living in oligotrophic waters. Heavier coral $\delta^{15}N$ values pinpoint not only site-specific eutrophication, but also a sewage nitrogen source enriched in ^{15}N. Our results show that eutrophication of reef seawater by land-based sources of pollution can

This article has been accepted for publication and undergone full peer review but has not been through the copyediting, typesetting, pagination and proofreading process which may lead to differences between this version and the Version of Record. Please cite this article as doi: 10.1002/2017JC013264

Received: Jul 12, 2017; Revised: Sep 13, 2017; Accepted: Sep 15, 2017

magnify the effects of OA through nutrient driven-bioerosion. These conditions could contribute to the collapse of coastal coral reef ecosystems sooner than current projections predict based only on ocean acidification.

1. Introduction

Coral reefs occupy less than 1% of the world's seafloor yet support hundreds of thousands of animal and plant species (Reaka-Kudla, 1987), sustain the livelihoods of hundreds of millions of people around the world, and protect thousands of kilometers of coastline from coastal hazards (Hughes *et al.*, 2003; Ferrario *et al.*, 2014). Yet coral reefs are facing increasing stress from global climate change, such as increasing temperatures, sea levels, and ocean acidification (OA), combined with local stresses from over-fishing, sedimentation, and land-based sources of pollution including coastal acidification (Knowlton and Jackson, 2008). As discussed in early work by Stearn et al. (1977), and Scoffin et al. (1980) on carbonate budgets, the carbonate accretion of coral reefs depends on two overarching processes: production of calcium carbonate ($CaCO_3$) skeletons by plants and animals on the reef and cementation of sand and rubble, and $CaCO_3$ breakdown and removal that occurs through bioerosion, dissolution, and offshore transport (e.g., Perry *et al.*, 2013; Glynn and Manzello, 2015). Accretion of $CaCO_3$ must exceed removal for modern reefs to be in a state of net growth. However, any factor facilitating the decrease of carbonate production could tip this balance, causing reefs to shift to a state of net loss. There is now strong evidence that calcification rates tend to decrease, and bioerosion and dissolution rates tend to increase with declining seawater pH and [CO_3^{2-}] (Hughes *et al.*, 2007; Anthony *et al.*, 2008; Enochs *et al.*, 2016). Under elevated aqueous pCO_2 (750 μatm) treatments, biogenic dissolution by euendolith (microborers) communities were found to yield a dissolution rate of 39 g $CaCO_3$ m^{-2} mo^{-1} (468 m□□□□□□ □□□□□ (Tribollet *et al.*, 2009). This is consistent with field observations from Oahu where bioerosion rates were highly sensitive to ocean pH (Silbiger *et al.*, 2014; Silbiger *et al.*, 2016). Nutrient loading can also accelerate bioerosion rates (Holmes *et al.*, 2000;

Carreiro-Silva *et al.*, 2005, 2009), as revealed at sites that were exposed to inorganic nutrient loading in the absence of macrograzers having bioerosion rates enriched by a factor of 10 (Carreiro-Silva *et al.*, 2005). Therefore, past studies indicate that both OA and nutrient loading separately can increase bioerosion rates. However, there is now compelling evidence that sensitivity to bioerosion is much magnified under multiple stressors, including stressors from nutrient and sediment loading, along with overfishing (Ban *et al.*, 2014; Vega Thurber *et al.*, 2014; DeCarlo *et al.*, 2015). Recently, DeCarlo et al. (2015) found macrobioerosion rates 10 times greater under high-nutrient conditions. Bioerosion rates of corals collected from naturally low pH environments were 10 times faster under nutrient rich (eutrophic) conditions compared with nutrient poor (oligotrophic) conditions. Although this observation was made on pristine, unpolluted reef systems, it highlights the potential dangers of nutrients to magnifying OA effects. This is of particular concern to coral reefs adjacent to densely inhabited shorelines, where nutrient fluxes can be high due to upstream fertilized, agricultural lands, treated wastewater injection, and leakage from leech field and septic systems close to shore.

Situated in the North Pacific Subtropical Gyre, the coral reef islands of Hawaii occupy a tropical, oligotrophic region with naturally occurring, low nutrient concentrations. On the Hawaiian island of Maui, however, anthropogenic nutrient loading to coastal waters via sustained submarine groundwater discharge (SGD) has been well documented (Dailer *et al.*, 2010; Dailer *et al.*, 2012; Bishop *et al.*, 2015; Amato *et al.*, 2016; Fackrell *et al.*, 2016). SGD consists of both terrestrial groundwater and recirculated seawater that is influenced by tides and waves (Dimova *et al.*, 2012). In Hawaii, where rivers are not abundant and permeability is high within the basaltic bedrock, SGD is an important water-borne transport vector for nutrients into the coastal ocean (Bienfang, 1980; Parsons *et al.*, 2008; Hunt and Rosa, 2009; Peterson *et al.*, 2009; Swarzenski *et al.*, 2012; Nelson *et al.*, 2015; Amato *et al.*, 2016; Fackrell *et al.*, 2016; Swarzenski *et al.*, 2016). As a result, SGD can impact the structure of marine biotic communities by delivering elevated nutrient loads that may lead to eutrophication, harmful algal blooms (Anderson *et al.*, 2002), decreased coral abundance and diversity,

and increased macroalgal abundance (Fabricius, 2005; Lapointe *et al.*, 2005), as well as low pH water that can cause coastal acidification (Wang *et al.*, 2014). Eutrophication, for example, from nitrogen and phosphorous pollution of land-based sources, such as septic leachate and fertilizers, can alter ecosystem function and structure by shifting reefs from being dominated by corals to being dominated by algae (Howarth *et al.*, 2000; Andrefouet *et al.*, 2002; Hughes *et al.*, 2007) and increasing the vulnerability of reefs to coral disease (Bruno *et al.*, 2003; Redding *et al.*, 2013).

"Dead zones," areas of clustered patches of variable degrees of degradation with discrete coral cover loss of nearly 100% have been observed for decades (Wiltse, 1996; Ross *et al.*, 2012) along the shallow coral reef at Kahekili in Kaanapali, west Maui, Hawaii, USA (Fig. 1). This area has a long history of macro-algal blooms (Smith *et al.*, 2005) and a decrease in herbivorous fishes attributed to overfishing (Williams *et al.*, 2016). As a result, there has been a shift over the past decades in benthic cover from abundant corals to turf- or macro-algae (Cochran *et al.*, 2014). Currently, only 51% of the hardbottom at Kahekili is covered with at least 10% live coral (Cochran *et al.*, 2014). Excessive algae growth has been a concern since the late 1980s, with potential links to input of nutrient-rich water via wastewater injection wells (Dailer *et al.*, 2010; Dailer *et al.*, 2012). Fluorescent dye tracer studies now confirm that there is a direct hydrologic link between the nearby Lahaina Wastewater Reclamation Facility (LWRF) and SGD, where treated wastewater is injected into groundwater that then flows towards the coast to emerge through a network of small seeps and vents (Glenn *et al.*, 2013; Swarzenski *et al.*, 2016). Changes in coastal water quality observed off west Maui can ultimately impact the balance between reef accretion and bioerosion, with reef degradation occurring through both the biological breakdown of the skeleton from microborers (e.g., alga and bacteria) and macroborers (e.g., bivalves and sponges; Osorno *et al.*, 2005) via mechanical and chemical bioerosion (see reviews by Tribollet and Golubic, 2011; Schönberg, 2017) as well as dissolution of $CaCO_3$ due to changes in the aragonite saturation state (Ω_{arag}) from both natural (Crook *et al.*, 2012; Crook *et al.*,

2013; Shamberger *et al.*, 2014; Silbiger *et al.*, 2014) and anthropogenic activities (Kleypas *et al.*, 1999; Hoegh-Guldberg *et al.*, 2007; Fabricius *et al.*, 2011).

We investigated the influence of SGD on reef biogeochemistry and growth of massive reef-building corals on a shallow reef at Kahekili in Kaanapali, west Maui, Hawaii, USA (Fig. 1), where the existence of numerous low salinity seeps provide a direct vector for low pH, nutrient-rich groundwater onto the reef (Glenn *et al.*, 2013; Swarzenski *et al.*, 2016). Sampling to characterize seawater chemistry at the primary seep site and in adjacent coastal waters was conducted in September 2014 and March 2016. Water samples were collected and analyzed for salinity, dissolved inorganic nutrients, and seawater carbonate system parameters (pH (total scale), total alkalinity (TA), and dissolved inorganic carbon (DIC)). The full seawater CO_2 system was calculated using the carbonate speciation program CO2SYS (Table S1; see methods). To investigate the response of corals to the combined effects of coastal acidification and nutrient loading associated with SGD, skeletal cores were extracted from *Porites lobata* corals located around the discharge seep (Fig. 1; Table 1), and to the north and south of its influence, and Computerized Tomography (CT) scanned at the Woods Hole Oceanographic Institution's Computerized Tomography Scanning Facility (Crook *et al.*, 2013). The scan images were analyzed for annual calcification and bioerosion rates using coralCT (DeCarlo and Cohen, 2016). With global warming and ocean acidification projected to compromise carbonate accretion (Hoegh-Guldberg *et al.*, 2007; Fabricius *et al.*, 2011; Gattuso *et al.*, 2015), managing the compounding effects from local stressors is a top priority in reef-management. Results from this work can therefore be used to estimate changes in coral reef health under future OA and shifting off continent material flux scenarios.

2. Methods

2.1 Coral growth parameters

Coral cores (n = 7) were collected in July 2013 from the shallow reef at Kahekili in Kaanapali, west Maui, Hawaii, from scleractinian *Porites lobata* (Fig. 1) in water depths of between 1 to 3 m and in the vicinity of brackish submarine groundwater discharge (SGD) "seeps" near Kahekili Beach Park (Glenn *et al.*, 2013), approximately 0.5 km southwest of the Lahaina Wastewater Reclamation Facility (LWRF) (Table 1). All cores were collected from living *Porites sp.*, except for adjacent to the vent where the coral colony was dead upon collection. Colonies were selected based on several criteria including distance from shore, distance from seep, coral shape, and water depth. Metrics of coral reef health (bioerosion, calcification, and growth rate) were quantified at the Woods Hole Oceanographic Institution's Computerized Tomography (CT) Scanning Facility (Crook *et al.*, 2013) where CT scan images (Fig. S1) were used to calculate the proportion of the skeleton eroded (>1 mm boring diameter) by boring organisms and calculated as the total volume of $CaCO_3$ removed relative to the total volume of the individual *Porites* coral core (Barkley *et al.*, 2015; DeCarlo *et al.*, 2015) using coralCT (DeCarlo and Cohen, 2016). The average growth rate reported in this study is the average linear extension rate and respective standard deviation for the length of cores analyzed per site. Pearson correlation coefficients and respective p-values were calculated in Excel. Significance levels were tested at the 95% and 90% confidence level. The number of years for analysis ranged from the upper 10 to 26 yr and was calculated as linear extension (mm) per yr. The range (i.e., length of core analyzed) reflects the fact that the quality/preservation of banding was not consistent across the collection sites due to differences in boring and erosion (Fig. S1). In comparison to measured bioerosion rates, predicted bioerosion rates were calculated using the equation from DeCarlo *et al.* (2015) where bioerosion rate = $-11.96 * \Omega_{arag} + 43.52$. Coral life spans were calculated based on annual growth rate and core length. Coral life span for the dead specimen was determined by comparing bomb-derived radiocarbon (^{14}C) values measured at 5 depth intervals to reference bomb-curves from Hawaii (Andrews *et al.*, 2016). Samples were prepared for Accelerator Mass Spectrometry (AMS) radiocarbon (^{14}C) dating at the National Ocean Sciences Accelerator Mass Spectrometry (NOSAMS) facility.

2.2 Carbonate geochemistry

Coral nitrogen isotope ($\delta^{15}N$) values were determined by collecting skeletal material (~300 mg) from the upper 4.0-5.6 mm of growth. Approximately 18 mg of material was placed into tin capsules with an approximately equivalent mass of vanadium oxide (V_2O_5) catalyst to ensure complete combustion for analysis using a Costech elemental analyzer - Isotope Ratio Mass Spectrometry (EA-IRMS) at the University of California at Santa Cruz and the USGS Stable Isotope Lab to determine $\delta^{15}N$ composition. Analytical uncertainty of 0.16 ‰ is reported based on replicate analysis of the international nitrogen standard, acetanilide.

2.3 Water sample collection and analysis

Sampling for water at the primary vent site and in adjacent coastal waters was conducted in September 2014 and March 2016. In 2014, sampling of the submarine springs was conducted using a piezometer point directly inserted into the primary vent site (Swarzenski *et al.*, 2012) and a 12V peristaltic pump during both high and low tide (Table S1). At each sampling site, the salinity and temperature of the vent water and bottom water was recorded using calibrated YSI multi-probes. Seawater sampling in March 2016 was conducted near the coral sites every 4-hr over a 6-d period for nutrients and carbonate chemistry variables. A peristaltic pump was used to pump seawater from the seafloor and temperature and salinity were recorded using a calibrated YSI multimeter. In-situ temperatures were also recorded from Solonist CTD Divers installed at each sampling tube (Prouty *et al.*, 2017).

Water samples were collected for the dissolved nutrients NH_4^+, Si, PO_4^{3-}, and [NO_3^-+NO_2^-] in duplicate, filtered with an in-line 0.45-μm filter (and 0.20 μm syringe filter for time-series sample), and kept frozen until analysis. Nutrients were analyzed at the Woods Hole Oceanographic Institution nutrient laboratory and University of California at Santa Barbara's Marine Science Institute Analytical

Laboratory via flow injection analysis for NH_4^+, Si, PO_4^{3-}, and [NO_3^-+ NO_2^-], with precisions of 0.6-3.0 %, 0.6-0.8 %, 0.9-1.3 %, and 0.3 %-1.0 % relative standard deviations, respectively. Nitrate isotope ($\delta^{15}N$ and $\delta^{18}O$) analyses were done at the University of California at Santa Cruz using the chemical reduction method (McIlvin and Altabet, 2005; Ryabenko *et al.*, 2009) and University of California at Davis' Stable Isotope Facilities using the denitrifier method (Sigman *et al.*, 2001). Using a Thermo Finnigan MAT 252 coupled with a GasBench II interface, isotope values are presented in per mil (‰) with respect to AIR for $\delta^{15}N$ and VSMO for $\delta^{18}O$ with a precision of 0.3-0.4‰ and 0.5-0.6‰ for $\delta^{15}N$-nitrate and $\delta^{18}O$-nitrate, respectively.

Measurement for carbonate chemistry parameters from the March 2016 collection were collected and analyzed for pH (total scale), TA, and DIC. A peristaltic pump was used to pump seawater from sampling sites through a 0.45-μm filter. Samples for pH were filtered into 30 mL optical glass cells, and were analyzed within 1 h of collection using spectrophotometric methods (Zhang and Byrne, 1996), an Ocean Optics USB2000 spectrometer and thymol blue indicator dye. Samples for TA (±1 μmol kg^{-1}) and DIC (±2 μmol kg^{-1}) were filtered into 300 ml borosilicate glass bottles, preserved by adding 100 uL saturated $HgCl_2$ solution, and bottles were pressured sealed with ground glass stoppers coated with Apiezpon grease. TA samples were analyzed using spectrophotometric methods of Yao and Byrne (1998) with an Ocean Optics USB2000 spectrometer and bromocresol purple indicator dye. DIC samples were analyzed using a UIC carbon coulometer model CM5014 and CM5130 acidification module fitted with a sulfide scrubber, and methods of Dickson *et al.* (2007). Dissolved oxygen (±0.1 mg L^{-1}), temperature (± 0.01°C), and salinity (± 0.01) were measured using a YSI multimeter calibrated daily. However, due to temperature change during water transit time within the sampling tube, in-situ temperatures as recorded from Solonist CTD Divers were reported and used to temperature corrected pH and perform CO2SYS calculations.

Certified reference materials (CRM) for TA and DIC analyses were from the Marine Physical Laboratory of Scripps Institution of Oceanography (person. Comm. A. Dickson). Duplicate or

triplicate analyses were performed on at least 10 % of samples, yielding a mean precision of ~1 μmol kg^{-1} and ~2 μmol kg^{-1} for TA and DIC analyses, respectively. For low salinity (<10) water samples collected directly from the vent, discrete DIC samples were measured on an Apollo SciTech AS-C3 DIC autoanalyzer via sample acidification followed by non-dispersive infrared CO_2 detection using a LiCOR 7000. The instrument was calibrated with certified reference material (CRM) from Dr. A.G. Dickson at the Scripps Institution of Oceanography. A modified Gran titration procedure by Wang and Cai (2004) was used to determine TA with an Apollo SciTech AS-ALK2 automated titrator and CRM-calibrated HCl at 25.0°C. The full seawater CO_2 system was calculated with measured salinity, temperature, nutrients (phosphate and silicate), TA, and pH data using an Excel Workbook Macro translation of the original CO2SYS program (Pierrot *et al.*, 2006). The CO2SYS 2.0 program was run with dissociation constants K_1 and K_2 from Mehrbach *et al.* (1973) refit by Dickson and Millero (1987) and KSO4 from Dickson (1990). The aragonite saturation state (Ω_{arag}) was defined as the ratio of $[CO_3^{2-}]$ and $[Ca^{2+}]$ divided by the aragonite solubility product (K_{sp}). The concentration of calcium $[Ca^{2+}]$ was assumed to be proportional to the salinity, and the carbonate concentration was calculated from DIC, pH, and the values of K_1 and K_2 (Pierrot *et al.*, 2006).

3. Results

3.1 Seawater carbonate chemistry

The 6-d continuous sampling in March 2016 revealed dynamic changes in the chemistry of seawater adjacent to the primary seep site, and captured the level of exposure of corals to variable pH and nutrient conditions (Fig 2; Table S1). From 16-19 March 2016, salinity increased and nutrient concentrations steadily declined, while pH values increased. From 21-24 March 2016, salinity decreased and nutrient concentrations increased by five orders of magnitude as pH fell, reaching values as low as 7.36 at the primary vent site (Fig. 2a,b). During this time, DIC and TA values increased, and Ω_{arag} fell below saturation for approximately 15 % of the time at the primary vent site (Fig. 2c, Table

S1). All carbonate parameters adjacent to the primary seep site behaved conservatively with respect to salinity (Fig. S2), demonstrating the tight coupling between nutrients and pH and freshened seep water input, consistent with earlier work documenting lower pH, nutrient enriched SGD derived seep water (Swarzenski *et al.*, 2012; Glenn *et al.*, 2013; Swarzenski *et al.*, 2016). Nutrients, TA, and DIC continued to covary with salinity at values greater than 33, suggesting that these stressors may have greater potential to impact those corals away from the vent. Although the salinity was extremely low at the vent, by the time affected waters reach corals only meters away, it had become well mixed with respect to salinity, and most corals in the vicinity of the vent were experiencing salinities ranging from 34 to 36 (Table S1). However, nutrients can impact the corals "downstream" because they are assimilated rapidly, fueling productivity that was likely driving the bioerosion (e.g., Carreiro-Silva *et al.*, 2005, 2009). These conditions clearly demonstrate that SGD is the primary source of elevated bottom water nutrient concentrations and dramatically under-saturated seawater ($\Omega_{arag} < 1$), corresponding to seawater pCO_2 values greater than 1500 μatm (Fig 2).

3.2 Coral cores

Measured bioerosion rates and percent volume erosion were highest at the coral site adjacent to the active SGD seep, and lowest at the coral site furthest from the seep, with bioerosion rates ranging between 23-99 mg cm^{-2} yr^{-1} (Table 2). However, the bioerosion rate of LobataHead06 may be an overestimate given that the core was collected from a dead specimen. The correlation between coral bioerosion rates and percent volume erosion relative to distance to the vent (r = -0.69 and -0.62; respectively) was significant at the 90% confidence level (Table 3). In addition, correlations between bioerosion rate and percent bioerosion volume and seawater parameters ($\Omega_{arag,}$ pH, and nitrate) were statistically significant ($p < 0.05$). Growth rates ranged from 0.69±0.10 cm yr^{-1} to 1.17±0.26 cm yr^{-1}, and calcification rates ranged from 0.67 to 1.10 g cm^{-2} yr^{-1} (Table 2). Calcification rates were

correlated to distance from shore (r = 0.72; $p \leq 0.05$; Table 3). Neither growth parameter, however, was statistically correlated to bioerosion rates or seawater parameters.

To investigate whether the corals assimilate SGD nitrate, the nitrogen isotope ($\delta^{15}N$) composition of the coral tissue from the upper 4.0-5.6 mm of coral growth was analyzed. Coral $\delta^{15}N$ values were highest closest to the seep site (17.08 ± 0.40 ‰; Table 2), and decreased with distance away from the vent (r = -0.58; p =0.09) and from shore (r = -0.88; p < 0.05; Table 3). With the exception of one coral head, all tissue $\delta^{15}N$ collected from corals near the primary seep zone, referred to as the "dead zone," were enriched relative to the north and south coral sites according to a one-way analysis of variance (ANOVA; $F_{(6,50)}$ =136.1; p < 0.0001; Fig. S3). Coral $\delta^{15}N$ values were also positively correlated to percent volume bioerosion (r = 0.68, p = 0.07; Fig. S3), and inversely correlated with calcification rates (r = -0.70, p = 0.06; Table 3).

4. Discussion

At the Kahekili site off the west coast of Maui, sustained SGD is rich in nutrients and also has lower pH (average 7.5±1.7). As a result of this SGD, the surrounding corals are exposed to multiple associated stressors, including nitrate concentrations up to 50 times higher than ambient seawater, and lower pH bottom water. Additional stressors from SGD, including reduced salinity at the primary vent site, and elevated TA and DIC concentrations can impact the corals by changes in photosynthesis, respiration, as well as increased bleaching and mortality (e.g. Ferrier-Pages *et al.*, 1999). We did not observe, however, the salinity extremes away from the vent that would have caused physiological stress/tissue loss/damage, yet increased rates of bioerosion were observed. An increase in TA and DIC can drive a shift from positive net community calcification to net negative community calcification, or net dissolution relative to calcification (Deffeyes, 1965). With expected reductions in calcification rates predicted under higher pCO_2 conditions (Shamberger *et al.*, 2011; Shaw *et al.*, 2012; Bernstein *et*

al., 2016), the interplay of bioeroding organisms under reduced community calcification could enhance both chemical and mechanical bioerosion rates.

Bioerosion rates from dead pieces of the massive coral *Porites* sp. skeleton from along a natural pH gradient in Kāneʻohe Bay, Oahu, reported rates from 2 to 91 g cm^{-2} yr^{-1} (Silbiger *et al.*, 2016), with the upper range in rates comparable to those observed closet to the SGD vent at Kahekili. Comparing bioerosion rates remains difficult, however, due to heterogeneity in bioeroding communities (e.g., chemical vs. mechanical, internal vs. external, micro- vs. macrobioeroders), as well as differences in environmental factors (e.g., hydrodynamics, temperature, etc.) and analytical approaches (e.g., SEM, grazing scars). For example, comparing bioerosion rates from carbonate blocks may not be an appropriate comparison given different bioeroding communities of dead versus alive substrate (e.g., (Hutchings, 1986; Sammarco *et al.*, 1987). In order to reduce uncertainty that could be an artifact from different field and/or analytical approach, rates derived by the same techniques as reported here were compared. Bioerosion rates from 15 sites across the tropical Pacific range from 0 to 68 mg cm^{-2} yr^{-1} (Table S2), with bioerosion rates at Kahekili up to 30 mg cm^{-2} yr^{-1} higher than measured elsewhere in the basin. Elevated bioerosion rates at Kahekili are consistent with findings from Sylbiger *et al.* (2017) that reported the highest average bioerosion rate and lowest net accretion rate across the Hawaiian Archipelago at the Kahekili study site. In comparison to measured bioerosion rates, we calculated predicted bioerosion rates using the equation from DeCarlo *et al.* (2015) where bioerosion rate = $-11.96 * \Omega_{arag} + 43.52$. Based on this computation, greater-than-predicted bioerosion rates for an oligotrophic setting in the Pacific were measured at Kahekili (Fig. 3). In other words, measured coral bioerosion rates at Kahekili are up to 8 times greater than expected for corals growing away from land-based sources of pollution (DeCarlo *et al.*, 2015) (Table 2).

Although our study did not quantify bioerosion rates by microborers *per se*, chemical bioerosion by microborers will contribute to net bioerosion rates by weakening of coral skeleton (Tribollet *et al.*, 2009) as well as by grazing from by fish and echinoids (Perry *et al.*, 2014). Given the

elevated nutrient concentrations at Kahekili, the data appear to indicate that eutrophication is driving elevated bioerosion rates at Kahekili. This finding is consistent with previous work showing increased bioeroding communities with increased nutrient concentrations and declining water quality (e.g., (Edinger *et al.*, 2000; Holmes *et al.*, 2000; Carreiro-Silva *et al.*, 2005, 2009). At Kahekili, large-scale ephemeral blooms of green alga (Smith *et al.*, 2005) can act to stimulate bioeroders, with both filter feeders and photoautotrophs capitalizing on nutrients in both the dissolved and particulate form. Microbioeroders can therefore interact with different bioeroding communities and contribute to the bioerosion loop (Schönberg, 2017). It is also important to point out the succession dynamics of bioeroders on marine carbonate budgets, whereby one taxon group prepares the substrate for the next bioeroder community (e.g., Hutchings 1986, 2011; Kiene and Hutchings, 1994; Scott 1988), including providing crevices for the intrusion of bivalves (e.g., Morton and Scott, 1980; Morton 1983). In addition, endolithic algae play an important role in erosive and early digenetic process (e.g., Kobluk and Risk, 1977; Kobluk and James, 1979). Vulnerability to physical erosion is further enhanced by bioerosion whereby the coral colony's ability to withstand wave shock and storm waves is reduced (e.g., Hein and Risk, 1975; Tunnicliffe 1979; 1981; Highsmith et al., 1980; Scott and Risk 1988). The degree of degradation and coral mortality has been linked to turf algal competition, with the "dead zone" characterized by clustered patches of variable degrees of degradation along the length of the reef at Kahekili Beach Park (Ross *et al.*, 2012). Increased mortality will therefore further facilitate bioerosion by increasing exposed carbonate structure on the corals. The decrease in abundance of reef grazing herbivores at Kahekili (Williams *et al.*, 2016) may also be a contributing factor to the establishment of certain bioeroders (Paddack *et al.*, 2006).

Elevated coral $\delta^{15}N$ values indicate not only eutrophication, but also a sewage nitrogen source enriched in ^{15}N (Heaton, 1986). Input of such an effluent to Maui's coral reef ecosystem has been documented by elevated algae $\delta^{15}N$ values, with the highest algae $\delta^{15}N$ values found adjacent to the

LWRF, yielding values of up to 43.3 ± 0.08‰, indicative of wastewater effluent (Dailer *et al.*, 2010). Those results are consistent with seawater δ^{15}N-nitrate values measured near the seep that were typically greater than 65‰ (Fig. 2a). The elevated coral and nitrate δ^{15}N ratios are therefore a function of both denitrification processes within the SGD pathway and an elevated δ^{15}N signature of the effluent source (Kendall, 1998; Fackrell *et al.*, 2016). The LWRF processes approximately 12.8 million L d^{-1} of wastewater effluent with estimated nitrogen loading of 79-97 kg d^{-1} (Glenn *et al.*, 2013). Based on SGD rates derived for the primary vent site (Swarzenski *et al.*, 2016) and nitrate concentrations measured directly from the discharging seep water (Table S1), the freshened seep water is estimated to deliver approximately 714 mol d^{-1} nitrate. Although seawater above the seep is an admixture of SGD and ambient seawater, exposure of nutrient-laden/low pH freshwater occurred approximately 8 hr d^{-1}, during the semidiurnal low tides when salinity values typically dropped below 10 and maximum SGD rates were observed (Glenn *et al.*, 2013). To exacerbate the exposure to contaminated nutrient-enriched effluent, the direction of maximum flow during the transition from high to low tide were dominantly offshore (Swarzenski *et al.*, 2016), transporting nutrient-rich water from the nearshore seeps towards the reef.

The elevated coral δ^{15}N values not only indicate that coral δ^{15}N appears to be a reliable tracer of nutrient loading and nitrate assimilation, but also further demonstrates a link between exposure to elevated nutrient levels and coral health given the observed increased bioerosion rates and decreased calcification rates at sites closest to the primary seep. In comparison, coral bioerosion rates and δ^{15}N values were lower at sites away from the primary seep, consistent with a decrease in nitrate flux (245 mol dy^{-1}) 85 m offshore from the primary seep site where measured SGD rates decreased to 30 cm d^{-1} (Swarzenski *et al.*, 2016). Enhanced nutrient loading from greater SGD nitrate fluxes can therefore increase abundance of bioeroding communities (Edinger *et al.*, 2000; Holmes *et al.*, 2000; Carreiro-Silva *et al.*, 2005, 2009). Teasing apart the different stressors from SGD is difficult given that pH,

nutrients, TA, and DIC covary with salinity. Any stressor that reduces live tissue coverage can ultimately increase bioerosion rates due to increased area of exposed substrate. At a salinity greater than 33, however, the relation between pH and salinity seems to break down, whereas TA, DIC, and nutrients continue to covary with salinity (Fig. S2), indicating that these stressors may have greater potential to impact corals growing away from the vent. Mesocosm experiments that can manipulate these individual stressors in a controlled environment (Wiedenmann *et al.*, 2013) therefore represent important complimentary studies to the field-based results presented here.

5. Conclusion

Based on observations from this site off west Maui, land-based sources of pollution, in synergy with changing ocean conditions on a global scale, interact to deleteriously influence coral reef health in the nearshore environment. Our results confirm how valuable nearshore coral reef ecosystems – the cornerstone of Hawaiian tourism, shoreline protection, and local fisheries – are affected by land-based sources of pollution that are also magnified by effects of coastal acidification. The range of exposure of reefs living in the vicinity of the SGD vents at Kahekili are comparable to end of century pCO_2 projections (Fabricius *et al.*, 2011) (Fig. 2c). With the largest decrease in Ω projected for the tropics (Gattuso *et al.*, 2015), coral reefs are extremely vulnerable to CO_2-related threats given the synergistic drivers responsible for present day coral degradation. Bioerosion rates at our study site, however, are much greater than predicted for an oligotrophic setting, suggesting that eutrophication exacerbates ocean acidification and bioerosion of corals, causing coral reef collapse much sooner in the future than currently predicted (van Hooidonk *et al.*, 2014). With many of Maui's coral reefs in significant decline (Rodgers *et al.*, 2015; Yates *et al.*, 2017) and recent coral bleaching events leading to increased coral mortality (Sparks *et al.*, 2016), reducing any stressors at a local scale – especially ones that can be readily attenuated with proactive resource management of nutrients – is imperative to sustaining future coral reef ecosystems and planning for resiliency.

Figures

Figure 1 Location map of the island of Maui, Hawaii, USA, and the study area at Kahekili along west Maui. Bathymetric map (5-m contours) of study area showing coral coring locations and seawater sampling sites (blue triangles) along Kahekili, primary seep site (red circle), superimposed on distribution of percent coral cover versus sand. Computerized tomography (CT) images and respective photographs of coral cores collected at the primary seep site and north of the primary seep site, approximately 780 m north of the primary seep cluster at Kahekili.

Figure 2 Results of time-series of seawater chemistry variables over a 6-d period collected from bottom water near the seep site on the nearshore reef (20°56.31660', -156°41.59080') every 4 hr. (a) Dissolved nutrient (nitrate+nitrite, phosphate, and silicate) concentrations (μmol L^{-1}), and nitrate stable nitrogen isotopes (δ^{15}N-nitrate; ‰); (b) temperature corrected pH (total scale); and (c) calculated carbonate parameters for aragonite saturation state (Ω_{arag}) and pCO_2 (μatm; inverted) based on TA-pH pairwise and measured salinity, temperature, nutrients (phosphate and silicate) data. End-of-century projections according to the "business as usual" RCP8.5 scenario for pH (reduction by 0.4 units), Ω_{arag} (2.0), and pCO_2 (750 μatm) (Fabricius *et al.*, 2011).

Figure 3 Relationship between aragonite saturation state ($\Omega_{arag}\pm1\sigma$; inverted axis) measured in March 2016 and coral bioerosion (mg cm^{-2} yr^{-1}) from west Maui exposed to anthropogenic nutrient loading (black circles), naturally high- (open circles) and low-nutrient (grey diamonds) reefs across the Pacific Basin (Barkley *et al.*, 2015; DeCarlo *et al.*, 2015). The predicted bioerosion rate for Maui (black cross) was calculated using the equation bioerosion rate = $-11.96 * \Omega_{arag} + 43.52$ (DeCarlo *et al.*, 2015) and a calculated Ω value of 3.06 based on offshore sampling site (~70 m), south of the seep (~150 m) site with nitrate concentrations <0.20 μmol L^{-1}.

Acknowledgments:

This research was carried out as part of the US Geological Survey's Coral Reefs Project in an effort in the USA and its trust territories to better understand the effects of geologic and oceanographic processes on coral reef systems and were supported by the USGS Coastal and Marine Geology Program. The authors gratefully acknowledge the vital partnership and expert logistics support provided by the State of Hawaii Division of Aquatic Resources. We thank N. Silbiger (UCI) for helpful discussion, K.R. Pietro and K. Hoering (WHOI), J. Murray (UCSC), S. Peek (USGS), C. Moore (USGS), and G. Paradis (UCSB) analytical assistance, and P. Dal Ferro, J. Logan, T. Reiss, and N. Smiley (USGS), J. McClaren (Stanford), M. Dailer (U. Hawaii), and C. Gallagher (UCSC) for field assistance, and S. Cochran (USGS) for assistance with figure. The IAEA is grateful for the support provided to its Environment Laboratories by the Government of the Principality of Monaco. The use of trade names is for descriptive purposes only and does not imply endorsement by the U.S. Government. We thank L. Robbins (USGS) and M. Risk (McMaster University) for providing helpful comments that greatly improved the manuscript. Additional data to support this project can be found in Prouty *et al.* (2017).

References:

Amato, D.W., Bishop, J.M., Glenn, C.R., Dulai, H., Smith, C.M., 2016. Impact of submarine groundwater discharge on marine water quality and reef biota of Maui. PLoS ONE 11 (11), e0165825, doi:10.1371/journal.pone.0165825

Anderson, D.M., Glibert, P.M., Burkholder, J.M., 2002. Harmful algal blooms and eutrophication: nutrient sources, composition and consequences. Estuaries 25, 562–584, doi:10.1007/BF02804901

Andrefouet, S., Mumby, P.J., McField, M., Hu, C., Muller-Karger, F.E., 2002. Revisiting coral reef connectivity. Coral Reefs 21 (1), 43-48, doi:10.1007/s00338-001-0199-0

Andrews, A.H., Siciliano, D., Potts, D.C., DeMartini, E.E., Covarrubias, S., 2016. Bomb radiocarbon and the Hawaiian Archipelago: coral, otoliths, and seawater. Radiocarbon 58 (3), 531-548, doi:10.1017/RDC.2016.32

Anthony, K.R.N., Kline, D.I., Diaz-Pulido, G., Dove, S., Hoegh-Guldberg, O., 2008. Ocean acidification causes bleaching and productivity loss in coral reef builders. Proceedings of the National Academy of Sciences 105 (45), 17442-17446, doi:10.1073/pnas.0804478105

Ban, S.S., Graham, N.A.J., Connolly, S.R., 2014. Evidence for multiple stressor interactions and effectson coral reefs. Global Change Biology 20 (3), 681-697, doi:10.1111/gcb.12453

Barkley, H.C., Cohen, A.L., Golbuu, Y., Starczak, V.R., DeCarlo, T.M., Shamberger, K.E.F., 2015. Changes in coral reef communities across a natural gradient in seawater pH. Science Advances 1 (5), doi:10.1126/sciadv.1500328.

Bernstein, W.N., Hughen, K.A., Langdon, C., McCorkle, D.C., Lentz, S.J., 2016. Environmental controls on daytime net community calcification on a Red Sea reef flat. Coral Reefs 35 (2), 697-711.

Bienfang, P., 1980. Water quality characteristics of Honokohau Harbor: A subtropical embayment affected by groundwater intrusion. Pacific Science 34 (3), 279-291.

Bishop, J.M., Glenn, C.R., Amato, D.W., Dulai, H., 2015. Effect of land use and groundwater flow path on submarine groundwater discharge nutrient flux. Journal of Hydrology: Regional Studies. doi:10.1016/j.ejrh.2015.10.008

Bruno, J.F., Petes, L.E., Harvell, C.D., Hettinger, A., 2003. Nutrient enrichment can increase the severity of coral diseases. Ecology Letters 6, 1056-1061, doi:10.1046/j.1461-0248.2003.00544.x

Carreiro-Silva, M., McClanahan, T.R., Kiene, W.E., 2005. The role of inorganic nutrients and herbivory in controlling microbioerosion of carbonate substratum. Coral Reefs 24 (2), 214-221, doi:10.1007/s00338-004-0445-3.

Carreiro-Silva, M., McClanahan, T.R., Kiene, W.E., 2009. Effects of inorganic nutrients and organic matter on microbial euendolithic community composition and microbioerosion rates. Marine Ecology Progress Series 392, 1-15.

Cochran, S.A., Gibbs, A.E., D.J., W., 2014. Benthic habitat map of the U.S. Coral Reef Task Force Watershed Partnership Initiative Kā‘anapali priority study area and the State of Hawai‘i Kahekili Herbivore Fisheries Management Area, west-central Maui, Hawai‘i. U.S. Geological Survey Open-File Report 2014-1129, p. 42 p.

Crook, E.D., Cohen, A.L., Rebolledo-Vieyra, M., Hernandez, L., Paytan, A., 2013. Reduced calcification and lack of acclimatization by coral colonies growing in areas of persistent natural acidification. Proceedings of the National Academy of Sciences 110 (27), 11044-11049, doi:10.1073/pnas.1301589110.

Crook, E.D., Potts, D., Rebolledo-Vieyra, M., Hernandez, L., Paytan, A., 2012. Calcifying coral abundance near low-pH springs: implications for future ocean acidification. Coral Reefs 31 (1), 239-245, oi:10.1007/s00338-011-0839-y.

Dailer, M.L., Knox, R.S., Smith, J.E., Napier, M., Smith, C.M., 2010. Using δ^{15}N values in algal tissue to map locations and potential sources of anthropogenic nutrient inputs on the island of Maui, Hawai‘i, USA. Marine Pollution Bulletin 60 (5), 655-671, doi:10.1016/j.marpolbul.2009.12.021.

Dailer, M.L., Ramey, H.L., Saephan, S., Smith, C.M., 2012. Algal δ^{15}N values detect a wastewater effluent plume in nearshore and offshore surface waters and three-dimensionally model the plume across a coral reef on Maui, Hawai‘i, USA. Marine Pollution Bulletin 64 (2), 207-213, doi:10.1016/j.marpolbul.2011.12.004.

DeCarlo, T.M., Cohen, A.L., 2016. coralCT: software tool to analyze computerized tomography (CT) scans of coral skeletal cores for calcification and bioerosion rates. Zenodo.

DeCarlo, T.M., Cohen, A.L., Barkley, H.C., Cobban, Q., Young, C., Shamberger, K.E., Brainard, R.E., Golbuu, Y., 2015. Coral macrobioerosion is accelerated by ocean acidification and nutrients. Geology 43 (1), 7-10, doi:10.1130/G36147.1.

Deffeyes, K.S., 1965. Carbonate equilibra: A graphic and algebraic approach Limnology and Oceanography 10 (3), 412-426, doi:10.4319/lo.1965.10.3.0412.

Dickson, A.G., 1990. Thermodynamics of the dissociation of boric acid in synthetic seawater from 273.15 to 318.15 K. Deep Sea Research Part A. Oceanographic Research Papers 37 (5), 755-766, doi:10.1016/0198-0149(90)90004-F.

Dickson, A.G., Millero, F.J., 1987. A comparison of the equilibrium constants for the dissociation of carbonic acid in seawater media. Deep Sea Research Part A. Oceanographic Research Papers 34 (10), 1733-1743, doi:10.1016/0198-0149(87)90021-5.

Dickson, A.G., Sabine, C.L., Christian, J.R., 2007. Guide to best practices for ocean CO_2 measurements. PICES Special Publication 3, 191 pp.

Dimova, N.T., Swarzenski, P.W., Dulaiova, H., Glenn, C.R., 2012. Utilizing multichannel electrical resistivity methods to examine the dynamics of the fresh water–seawater interface in two Hawaiian groundwater systems. Journal of Geophysical Research: Oceans 117 (C2), doi:10.1029/2011jc007509.

Edinger, E.N., Limmon, G.V., Jompa, J., Widjatmoko, W., Heikoop, J.M., Risk, M.J., 2000. Normal coral growth rates on dying reefs: are coral growth rates good indicators of reef health? Marine Pollution Bulletin 40 (5), 404-425.

Enochs, I.C., Manzello, D.P., Kolodziej, G., Noonan, S.H.C., Valentino, L., Fabricius, K.E., 2016. Enhanced macroboring and depressed calcification drive net dissolution at high-CO_2 coral reefs. Proceedings of the Royal Society B: Biological Sciences 283 (1842), doi: 10.1098/rspb.2016.1742.

Fabricius, K.E., 2005. Effects of terrestrial runoff on the ecology of corals and coral reefs: review and synthesis. Mar Poll Bull 50, 125-146, doi:10.1016/j.marpolbul.2004.11.028.

Fabricius, K.E., Langdon, C., Uthicke, S., Humphrey, C., Noonan, S., De'ath, G., Okazaki, R., Muehllehner, N., Glas, M.S., Lough, J.M., 2011. Losers and winners in coral reefs acclimatized to elevated carbon dioxide concentrations. Nature Climate Change 1 (3), 165-169, doi:10.1038/nclimate1122.

Fackrell, J.K., Glenn, C.R., Popp, B.N., Whittier, R.B., Dulai, H., 2016. Wastewater injection, aquifer biogeochemical reactions, and resultant groundwater N fluxes to coastal waters: Kā'anapali, Maui, Hawai'i. Marine Pollution Bulletin 110 (1), 281-292, doi:10.1016/j.marpolbul.2016.06.050.

Ferrario, F., Beck, M.W., Storlazzi, C.D., Micheli, F., Shepard, C.C., Airoldi, L., 2014. The effectiveness of coral reefs for coastal hazard risk reduction and adaptation. Nature communications 5, doi:10.1038/ncomms4794.

Ferrier-Pages, C., Gattuso, J.P., Jaubert, J., 1999. Effect of small variations in salinity on the rates of photosynthesis and respiration of the zooxanthellate coral Stylophora pistillata. Marine Ecology Progress Series 181, 309-314.

Gattuso, J.P., Magnan, A., Billé, R., Cheung, W.W.L., Howes, E.L., Joos, F., Allemand, D., Bopp, L., Cooley, S.R., Eakin, C.M., Hoegh-Guldberg, O., Kelly, R.P., Pörtner, H.O., Rogers, A.D., Baxter, J.M., Laffoley, D., Osborn, D., Rankovic, A., Rochette, J., Sumaila, U.R., Treyer, S., Turley, C., 2015. Contrasting futures for ocean and society from different anthropogenic CO_2 emissions scenarios. Science 349 (6243), doi:10.1126/science.aac4722.

Glenn, C.R., Whittier, R.B., Dailer, M.L., Dulaiova, H., El-Kadi, A.I., Fackrell, J., Kelly, J.L., Waters, C.A., Sevadjian, L., 2013. Lahaina Groundwater Tracer Study – Lahaina, Maui, Hawaii, Final Report. State of Hawaii Department of Health, the U.S. Environmental Protection Agency, and the U.S. Army Engineer Research and Development Center, p. 502 p.

Glynn, P.W., Manzello, D.P., 2015. Bioerosion and coral reef growth: a dynamic balance. Coral reefs in the Anthropocene. Springer, pp. 67-97.

Heaton, T.H.E., 1986. Isotopic studies of nitrogen pollution in the hydrosphere and atmosphere: A review. Chemical Geology: Isotope Geoscience section 59, 87-102.

Hein, F.J., Risk, M.J., 1975. Bioerosion of coral heads: inner patch reefs, Florida reef tract. Bulletin of Marine Science 25 (1), 133-138.

Highsmith, R.C., Riggs, A.C., D'Antonio, C.M., 1980. Survival of hurricane-generated coral fragments and a disturbance model of reef calcification/growth rates. Oecologia 46 (3), 322-329.

Hoegh-Guldberg, O., Mumby, P.J., Hooten, A.J., Steneck, R.S., Greenfield, P., Gomez, E., Harvell, C.D., Sale, P.F., Edwards, A.J., Caldeira, K., Knowlton, N., Eakin, C.M., Iglesias-Prieto, R., Muthiga, N., Bradbury, R.H., Dubi, A., Hatziolos, M.E., 2007. Coral reefs under rapid climate change and ocean acidification. Science 318 1737-1742, doi:10.1126/science.1152509.

Holmes, K.E., Edinger, E.N., Limmon, G.V., Risk, M.J., 2000. Bioerosion of live massive corals and branching coral rubble on Indonesian coral reefs. Marine Pollution Bulletin 40 (7), 606-617.

Howarth, R., Anderson, D., Cloern, J., Elfring, C., Hopkinson, C., Lapointe, B., Malone, T., Marcus, N., McGlathery, K., Sharpley, A., Walker, D., 2000. Nutrient pollution of coastal rivers, bays, and seas. Issues in Ecology, 7, 1 – 15.

Hughes, T.P., Baird, A.H., Bellwood, D.R., Card, M., Connolly, S.R., Folke, C., Grosberg, R., Hoegh-Guldberg, O., Jackson, J.B.C., Kleypas, J., Lough, J.M., Marshall, P., Nystrom, M., Palumbi, S.R., Pandolfi, J.M., Rosen, B., Roughgarden, J., 2003. Climate change, human impacts, and the resilience of coral reefs. Science 301 (5635), 929-933, doi: 10.1126/science.1085046.

Hughes, T.P., Rodrigues, M.J., Bellwood, D.R., Ceccarelli, D., Hoegh-Guldberg, O., McCook, L., Moltschaniwskyj, N., Pratchett, M.S., Steneck, R.S., Willis, B., 2007. Phase shifts, serbivory, and the resilience of coral reefs to climate change. Current Biology 17 (4), 360-365, doi:10.1016/j.cub.2006.12.049.

Hunt, C.D., Jr., Rosa, S.N., 2009. A multitracer approach to detecting wastewater plumes from municipal injection wells in nearshore marine waters at Kihei and Lahaina, Maui, Hawaii. U.S. Geological Survey Scientific Investigations Report 2009-5253, p. 166 p.

Hutchings, P.A., 1986. Biological destruction of coral reefs. Coral Reefs 4 (4), 239-252, doi:10.1007/BF00298083.

Hutchings, P., 2011. Bioerosion. Encyclopedia of Modern Coral Reefs. Springer, pp. 139-156.

Kendall, C., 1998. Tracing nitrogen sources and cycling in catchments, In: Kendall, C., McDonnell, J.J. (Eds.), Isotope Tracers in Catchment Hydrology, Elsevier, Amsterdam, , pp. pp. 519-576.

Kiene, W.E., Hutchings, P.A., 1994. Bioerosion experiments at Lizard Island, Great Barrier Reef. Coral Reefs 13 (2), 91-98.

Kleypas, J.A., Buddemeier, R.W., Archer, D., Gattuso, J.-P., Langdon, C., Opdyke, B.N., 1999. Geochemical consequences of increased atmospheric carbon dioxide on coral reefs. Science 284 (5411), 118-120, doi:10.1126/science.284.5411.118.

Knowlton, N., Jackson, J.B.C., 2008. Shifting baselines, local impacts, and global change on coral reefs. PLoS Biol 6 (2), e54, doi:10.1371/journal.pbio.0060054.

Kobluk, D.R., James, N.P., 1979. Cavity - dwelling organisms in Lower Cambrian patch reefs from southern Labrador. Lethaia 12 (3), 193-218.

Kobluk, D.R., Risk, M.J., 1977. Calcification of exposed filaments of endolithic algae, micrite envelope formation and sediment production. Journal of Sedimentary Research 47 (2).

Lapointe, B.E., Barile, P.J., Littler, M.M., Littler, D.S., 2005. Macroalgal blooms on southeast Florida coral reefs. II. Cross-shelf $\delta^{15}N$ values provide evidence of widespread sewage enrichment. Harmful Algae 4, 1106–1122, doi:10.1016/j.hal.2005.06.004.

McIlvin, M.R., Altabet, M.A., 2005. Chemical conversion of nitrate and nitrite to nitrous oxide for nitrogen and oxygen isotopic analysis in freshwater and seawater. Analytical Chemistry 77 (17), 5589-5595, doi:10.1021/ac050528s.

Mehrbach, C., Culberson, C.H., Hawley, J.E., Pytkowicx, R.M., 1973. Measurement of the apparent dissociation constants of carbonic acid in seawater at atmospheric pressure. Limnology and Oceanography 18 (6), 897-907, doi:10.4319/lo.1973.18.6.0897.

Nelson, C.E., Donahue, M.J., Dulaiova, H., Goldberg, S.J., La Valle, F.F., Lubarsky, K., Miyano, J., Richardson, C., Silbiger, N.J., Thomas, F.I.M., 2015. Fluorescent dissolved organic matter as a multivariate biogeochemical tracer of submarine groundwater discharge in coral reef ecosystems. Marine Chemistry 177, Part 2, 232-243.

Osorno, A., Peyrot-Clausade, M., Hutchings, P.A., 2005. Patterns and rates of erosion in dead Porites across the Great Barrier Reef (Australia) after 2 years and 4 years of exposure. Coral Reefs 24 (2), 292-303.

Paddack, M.J., Cowen, R.K., Sponaugle, S., 2006. Grazing pressure of herbivorous coral reef fishes on low coral-cover reefs. Coral Reefs 25 (3), 461-472, doi:10.1007/s00338-006-0112-y.

Parsons, M.L., Walsh, W.J., Settlemier, C.J., White, D.J., Ballauer, J.M., Ayotte, P.M., Osada, K.M., Carman, B., 2008. A multivariate assessment of the coral ecosystem health of two embayments on the lee of the island of Hawai'i. Marine Pollution Bulletin 56 (6), 1138-1149, doi:10.1016/j.marpolbul.2008.03.004.

Perry, C.T., Murphy, G.N., Kench, P.S., Edinger, E.N., Smithers, S.G., Steneck, R.S., Mumby, P.J., 2014. Changing dynamics of Caribbean reef carbonate budgets: emergence of reef bioeroders as critical controls on present and future reef growth potential. The Royal Society, 281, doi: 10.1098/rspb.2014.2018

Perry, C.T., Murphy, G.N., Kench, P.S., Smithers, S.G., Edinger, E.N., Steneck, R.S., Mumby, P.J., 2013. Caribbean-wide decline in carbonate production threatens coral reef growth. Nature communications 4, 1402, doi:10.1038/ncomms2409

Peterson, R.N., Burnett, W.C., Glenn, C.R., Johnson, A.G., 2009. Quantification of point-source groundwater discharges from the shoreline of the Big Island, Hawaii. Limnol. Oceanogr. 54, 890–904, doi:10.4319/lo.2009.54.3.0890.

Pierrot, D., Lewis, E., Wallace, D.W.R., 2006. MS Excel program developed for CO_2 system calculations. ORNL/CDIAC-105a. Carbon Dioxide Information Analysis Center, Oak Ridge National Laboratory, US Department of Energy, Oak Ridge, Tennessee.

Prouty, N.G., Yates, K.K., Smiley, N.A., and Gallagher, C., 2017, Coral growth parameters and seawater chemistry, Kahekili, west Maui: U.S. Geological Survey data release, doi: 10.5066/F7X34VPV.

Reaka-Kudla, M.L., 1987. The global biodiversity of coral reefs: A comparison with rainforests. In: Reaka-Kudla, M.L., Wilson, D.E., Wilson, E.O. (Eds.), Biodiversity II: Understanding and Protecting Our Natural Resources. Joseph Henry/National Academy Press, Washington, D. C., pp. 83-108.

Redding, J.E., Myers-Miller, R.L., Baker, D.M., Fogel, M., Raymundo, L.J., Kim, K., 2013. Link between sewage-derived nitrogen pollution and coral disease severity in Guam. Marine Pollution Bulletin 73 (1), 57-63, doi:10.1016/j.marpolbul.2013.06.002.

Rodgers, K.u.S., Jokiel, P.L., Brown, E.K., Hau, S., Sparks, R., 2015. Over a decade of change in spatial and temporal dynamics of Hawaiian coral reef communities 1. Pacific Science 69 (1), 1-13, doi:10.2984/69.1.1.

Ross, M., White, D., Aiwohi, M., Walton, M., Sudek, M., Lager, D., Jokiel, P., 2012. Characterization of "dead zones" and population demography of Porites compressa along a gradient of anthropogenic nutrient input at Kahekili Beach Park, Maui. Final Report for Project C11722. State of Hawaii, Department of Land and Natural Resources, Division of Aquatic Resources, Honolulu, Hawaii 96813.

Ryabenko, E., Altabet, M.A., Wallace, D.W.R., 2009. Effect of chloride on the chemical conversion of nitrate to nitrous oxide for δ15N analysis. Limnology and Oceanography Methods 7, 545-552, doi:10.4319/lom.2009.7.545.

Sammarco, P.W., Risk, M.J., Rose, C., 1987. Effects of grazing and damselfish territoriality on internal bioerosion of dead corals : indirect effects. Journal of Experimental Marine Biology and Ecology 112 (2), 185-199, doi:10.1016/0022-0981(87)90116-X.

Schönberg, C.H., Fang, J. K., Carreiro-Silva, M., Tribollet, A., Wisshak, M., 2017. Bioerosion: the other ocean acidification problem: Contribution to the Themed Issue:'Ocean Acidification'. ICES Journal of Marine Science., doi:10.1093/icesjms/fsw254

Scoffin, T.P., Stearn, C.W., Boucher, D., Frydl, P., Hawkins, C., Hunter, I.G., MacGeachy, J.K., 1980. Calcium carbonate budget of a fringing reef on the west coast of Barbados: part II—erosion, sediments and internal structure. Bulletin of Marine Science 30, 475–508.

Scott, P.J.B., Risk, M.J., 1988. The effect of Lithophaga (Bivalvia: Mytilidae) boreholes on the strength of the coral Porites lobata. Coral Reefs 7 (3), 145-151.

Shamberger, K.E.F., Cohen, A.L., Golbuu, Y., McCorkle, D.C., Lentz, S.J., Barkley, H.C., 2014. Diverse coral communities in naturally acidified waters of a Western Pacific reef. Geophysical Research Letters 41 (2), 499-504, doi:10.1002/2013GL058489.

Shamberger, K.E.F., Feely, R.A., Sabine, C.L., Atkinson, M.J., DeCarlo, E.H., Mackenzie, F.T., Drupp, P.S., Butterfield, D.A., 2011. Calcification and organic production on a Hawaiian coral reef. Marine Chemistry 127 (1), 64-75.

Shaw, E.C., McNeil, B.I., Tilbrook, B., 2012. Impacts of ocean acidification in naturally variable coral reef flat ecosystems. Journal of Geophysical Research: Oceans 117 (C3).

Sigman, D.M., Casciotti, K.L., Andreani, M., Barford, C., Galanter, M., Bohlke, J.K., 2001. A bacterial method for the nitrogen isotopic analysis of nitrate in seawater and freshwater. Analytical Chemistry 73, 4145-4415, doi:10.1021/ac010088e.

Silbiger, N.J., Donahue, M.J., Brainard, R.E., Environmental drivers of coral reef carbonate production and bioerosion: a multi-scale analysis. Ecology, doi**:** 10.1002/ecy.1946

Silbiger, N.J., Guadayol, Ò., Thomas, F.I.M., Donahue, M.J., 2014. Reefs shift from net accretion to net erosion along a natural environmental gradient. Marine Ecology Progress Series 515, 33-44.

Silbiger, N.J., Guadayol, Ò., Thomas, F.I.M., Donahue, M.J., 2016. A Novel μCT analysis reveals different responses of bioerosion and secondary accretion to environmental Variability. PLoS ONE 11 (4), e0153058, doi:10.1371/journal.pone.0153058.

Smith, J.E., Runcie, J.W., Smith, C.M., 2005. Characterization of a large-scale ephemeral bloom of the green alga Cladophora sericea on the coral reefs of West Maui, Hawaii. Marine Ecology Progress Series 302, 77-91.

Sparks, R.T., Stone, K., White, D.J., Ross, M., Williams, I.D., 2016. Maui and Lanai Monitoring Report. Hawaii Department of Land and Natural Resources, Division of Aquatic Resources, Maui, 130 Mahalani Street, Wailuku HI. 96790.

Stearn, C.W., Scoffin, T.P., Martindale, W., 1977. Calcium Carbonate Budget of a Fringing Reef on the West Coast of BarbadosvPart I—Zonation and Productivitity. Bulletin of Marine Science 27, 479–510.

Swarzenski, P., Dulai, H., Kroeger, K., Smith, C., Dimova, N., Storlazzi, C., Prouty, N., Gingerich, S., Glenn, C., 2016. Observations of nearshore groundwater discharge: Kahekili Beach Park submarine springs, Maui, Hawaii. Journal of Hydrology: Regional Studies, doi:10.1016/j.ejrh.2015.12.056.

Swarzenski, P.W., Storlazzi, C.D., Presto, M.K., Gibbs, A.E., Smith, C.G., Dimova, N.T., Dailer, M.L., Logan, J.B., 2012. Nearshore morphology, benthic structure, hydrodynamics, and coastal groundwater discharge near Kahekili Beach Park, Maui, Hawaii:. U.S. Geological Survey Open-File Report 2012–1166, p. 34 p.

Tribollet, A., Godinot, C., Atkinson, M., Langdon, C., 2009. Effects of elevated pCO_2 on dissolution of coral carbonates by microbial euendoliths. Global Biogeochemical Cycles 23 (3), doi:10.1029/2008gb003286.

Tribollet, A., Golubic, S., 2011. Reef bioerosion: agents and processes. Coral Reefs: An Ecosystem in Transition. Springer, pp. 435-449.

Tunnicliffe, V., 1979. The role of boring sponges in coral fracture. Biologie des spongiaires 291, 309-315.

Tunnicliffe, V., 1981. Breakage and propagation of the stony coral Acropora cervicornis. Proceedings of the National Academy of Sciences 78 (4), 2427-2431.

van Hooidonk, R., Maynard, J.A., Manzello, D., Planes, S., 2014. Opposite latitudinal gradients in projected ocean acidification and bleaching impacts on coral reefs. Global Change Biology 20 (1), 103-112, doi:10.1111/gcb.12394.

Vega Thurber, R.L., Burkepile, D.E., Fuchs, C., Shantz, A.A., McMinds, R., Zaneveld, J.R., 2014. Chronic nutrient enrichment increases prevalence and severity of coral disease and bleaching. Global Change Biology 20 (2), 544-554, doi:10.1111/gcb.12450.

Wang, G., Jing, W., Wang, S., Xu, Y., Wang, Z., Zhang, Z., Li, Q., Dai, M., 2014. Coastal acidification induced by tidal-driven submarine groundwater discharge in a coastal coral feef system. Environmental Science & Technology 48 (22), 13069-13075, doi:10.1021/es5026867.

Wang, Z.A., Cai, W.-J., 2004. Carbon dioxide degassing and inorganic carbon export from a marsh-dominated estuary (the Duplin River): A marsh CO_2 pump. Limnology and Oceanography 49 (2), 341-354, doi:10.4319/lo.2004.49.2.0341.

Wiedenmann, J., D'Angelo, C., Smith, E.G., Hunt, A.N., Legiret, F.-E., Postle, A.D., Achterberg, E.P., 2013. Nutrient enrichment can increase the susceptibility of reef corals to bleaching. Nature Clim. Change 3 (2), 160-164, doi:10.1038/nclimate1661.

Williams, I.D., White, D.J., Sparks, R.T., Lino, K.C., Zamzow, J.P., Kelly, E.L.A., Ramey, H.L., 2016. Responses of Herbivorous Fishes and Benthos to 6 Years of Protection at the Kahekili Herbivore Fisheries Management Area, Maui. PLoS ONE 11 (7), e0159100, doi:10.1371/journal.pone.0159100.

Wiltse, W., 1996. Algal Blooms: Progress Report on Scientific Research. West Maui Watershed Management Project, State of Hawaii Department of Health, Honolulu. 64 pp.

Yao, W., Byrne, R.H., 1998. Simplified seawater alkalinity analysis: use of linear array spectrometers. Deep Sea Research Part I: Oceanographic Research Papers 45 (8), 1383-1392.

Yates, K.K., Zawada, D.G., Smiley, N.A., Tiling-Range, G., 2017. Divergence of seafloor elevation and sea level rise in coral reef ecosystems. Biogeosciences 14 (6), 1739-1772, doi:10.5194/bg-14-1739-2017.

Zhang, H., Byrne, R.H., 1996. Spectrophotometric pH measurements of surface seawater at in-situ conditions: absorbance and protonation behavior of thymol blue. Marine Chemistry 52 (1), 17-25, doi:10.1016/0304-4203(95)00076-3.

Author Contributions: N.P., P.S., and C.S. conceived and designed the research. N.P., K.Y., D.W., C.S., and P.S. collected the samples. N.P, A.C., and K.Y. analyzed the data. All the authors contributed to writing the manuscript and participated in the scientific discussion.

Additional Information

Supplementary information accompanies this paper.

Competing financial information: The authors declare no competing financial interests.

Coral ID	Core Length (cm)	Water Depth (m)	Lat	Long	Lifespan	Tissue thickness (mm)	Distance offshore (m)	Distance from seep (m)	Direction from seep (°)
LobataHead01	50	<2	20° 56.317'N	156° 41.598'W	1970-2013	5.13	38	15	264
LobataHead02	18	<2	20° 56.320'N	156° 41.605'W	1992-2013	5.63	52	29	279
LobataHead03	19	<2	20° 56.324'N	156° 41.594'W	1987-2013	4.63	33	15	324
LobataHead04	21	<2	20° 56.326'N	156° 41.587'W	1983-2013	4.00	20	16	16
LobataHead05	28	<2	20° 56.708'N	156° 41.590'W	1984-2013	4.63	58	783	0
LobataHead06	22	<1	20° 56.318'N	156° 41.589'W	1978-2008[1]	n/a	23	*at seep*	*at seep*
LobataHead07	50	3	20° 56.236'N	156° 41.611'W	n/a	5.13	68	156	194

1 - Age of death determined by bomb-derived ^{14}C value

Table 1 Location and physical characteristics of coral coring locations off Kahekili Beach Park collected in July 2013 from *Porites lobata*.

Coral Head	Growth Rate	Density	Calcification	Volume Bioerosion	Bioerosion Rate	Predicted bioerosion Rate	$\delta^{15}N$	Ω_{arag}	pH	Salinity	Nitrate
LobataHead01 (n=24 yrs)	1.17±0.26	1.04	1.10	6.57	72.32	n/a	11.29 ± 1.76 (n=9)	n/a	n/a	n/a	n/a
LobataHead02 (n=21 yrs)	0.88±0.06	1.08	0.94	5.94	56.03	7.04	8.44 ± 0.12 (n=12)	3.05±0.10	8.00±0.02	35.19±0.87	0.16±0.10
LobataHead03 (n=26 yrs)_	0.72±0.10	0.99	0.71	12.48	89.07	n/a	10.87 ± 0.45 (n=9)	n/a	n/a	n/a	n/a
LobataHead04 (n=20 yrs)	0.72±0.16	1.01	0.67	5.92	39.87	7.04	14.62 ± 0.23 (n=9)	3.05±0.17	8.01±0.03	34.98±0.99	0.41±0.18
LobataHead05 (n=13 yrs)	0.95±0.11	1.15	1.02	2.20	22.58	6.92	7.50 ± 0.19 (n=9)	3.06±0.11	8.01±0.02	35.36±1.10	0.19±0.11
LobataHead06 (n=10 yrs)	0.69±0.10	1.07	0.68	14.63	99.15	16.37	17.08 ± 0.40 (n=3)	2.27±0.81	7.85±0.17	28.57±7.79	20.35±23.32

LobataHead07	n/a	n/a	n/a	n/a	n/a	n/a	8.17 ± 0.19 (n=6)	n/a	n/a	n/a	n/a

Table 2 Coral growth parameters quantified by computerized tomography (CT) for growth rate (±SD; (cm yr^{-1}), density (g cm^{-3}), and calcification rates (g cm^{-2} yr^{-1}), percent volume erosion (%), measured bioerosion rate (mg cm^{-2} yr^{-1}), predicted bioerosion rate (mg cm^{-2} yr^{-1}) based on (DeCarlo *et al.*, 2015); bioerosion rate = -11.96* Ω_{arag} + 43.52), and average (±STD) coral tissue nitrogen isotope ($\delta^{15}N$; (‰) values. LobataHead07 was not analyzed for growth parameters prior to subsectioning for geochemical analysis. Seawater chemistry parameters ($\Omega_{arag,}$ temperature corrected-pH, salinity, and nitrate (μmol L^{-1}) are reported as average (±SD; *n* = 37) based on 6-d sampling period in March 2016.

	Coral Tissue $\delta^{15}N$	Growth Rate	Density	% Volume bioerosion	Calcification	Bioerosion rate	Lifespan	Distance from shore	Distance from seep	$\Omega_{arag,}$	pH
Average Growth Rate	**-0.53**										
Overall density	**-0.45**	**0.33**									
Bioerosion % volume	***0.68***	**-0.57**	**-0.51**								
Average Calcification	***-0.70***	0.95	**0.54**	***-0.66***							
Bioerosion Rate	**0.55**	**-0.27**	**-0.51**	0.94	**-0.39**						
Lifespan	**0.29**	***0.60***	**-0.09**	**0.02**	**0.38**	**0.20**					
Distance from shore	-0.88	**0.49**	0.81	***-0.68***	0.72	***-0.61***	**-0.22**				

Distance from seep	***-0.58***	**0.26**	0.80	***-0.62***	**0.44**	***-0.69***	**-0.08**	0.83			
$\Omega_{arag,}$	**-0.66**	**0.64**	**0.05**	-0.95	**0.57**	-0.91	**-0.55**	**0.53**	**0.37**		
pH	**-0.72**	**0.62**	**0.05**	-0.95	**0.54**	-0.93	**-0.50**	**0.50**	**0.39**	0.99	
Nitrate	**0.74**	**-0.64**	**-0.05**	0.94	**-0.57**	0.91	**0.56**	**-0.53**	**0.36**	0.99	0.99

Table 3 Pearson-product correlation coefficients (r; bold $p \leq 0.05$; italics $p \leq 0.10$) between average coral reef growth parameters (growth rate, density, %volume bioerosion, calcification, and lifespan), location (distance from shore and primary seep site), average coral δ^{15}N-nutrient loading proxy, and average seawater variables ($\Omega_{arag,,}$ pH, and nitrate).

Figure 1.

Figure 1

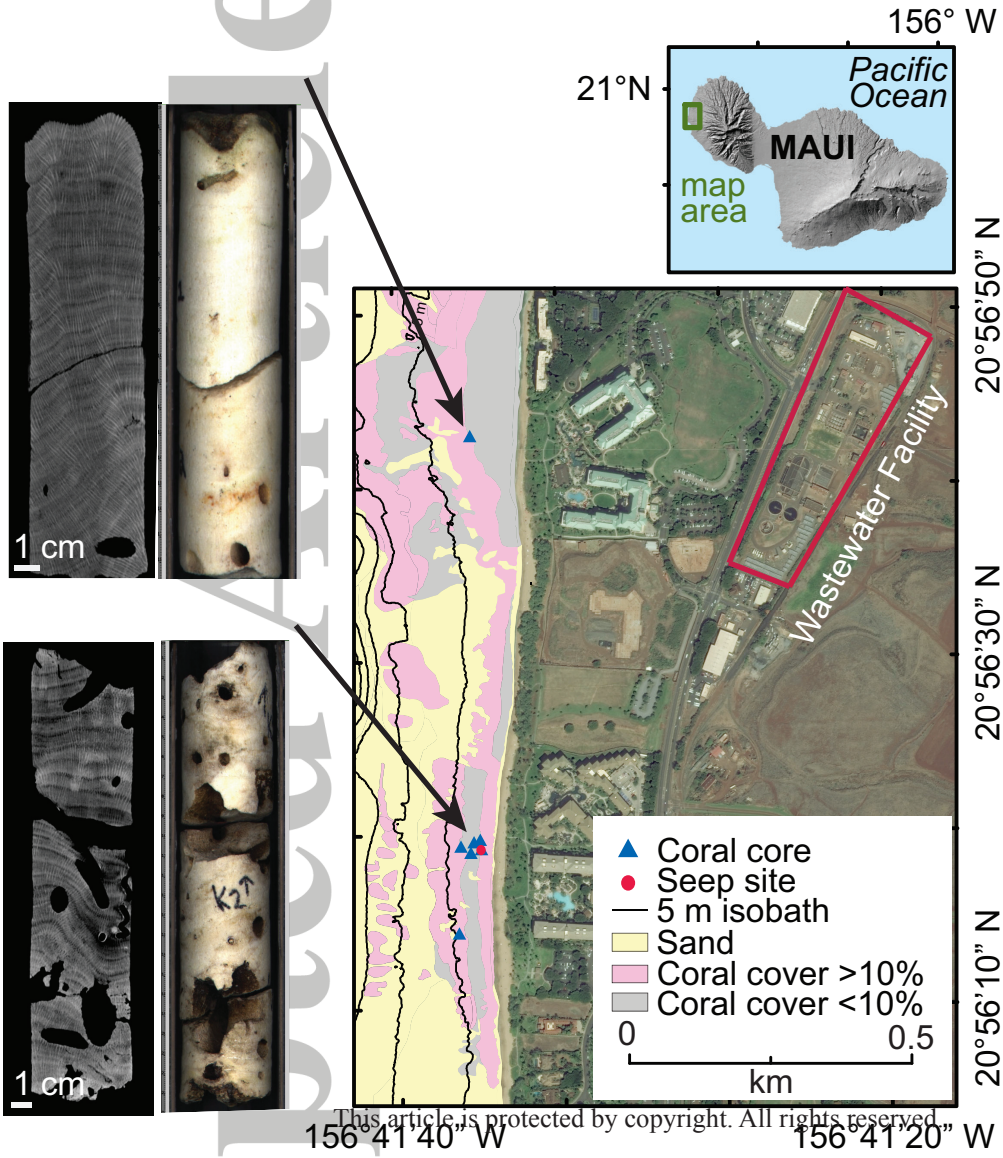

Figure 2.

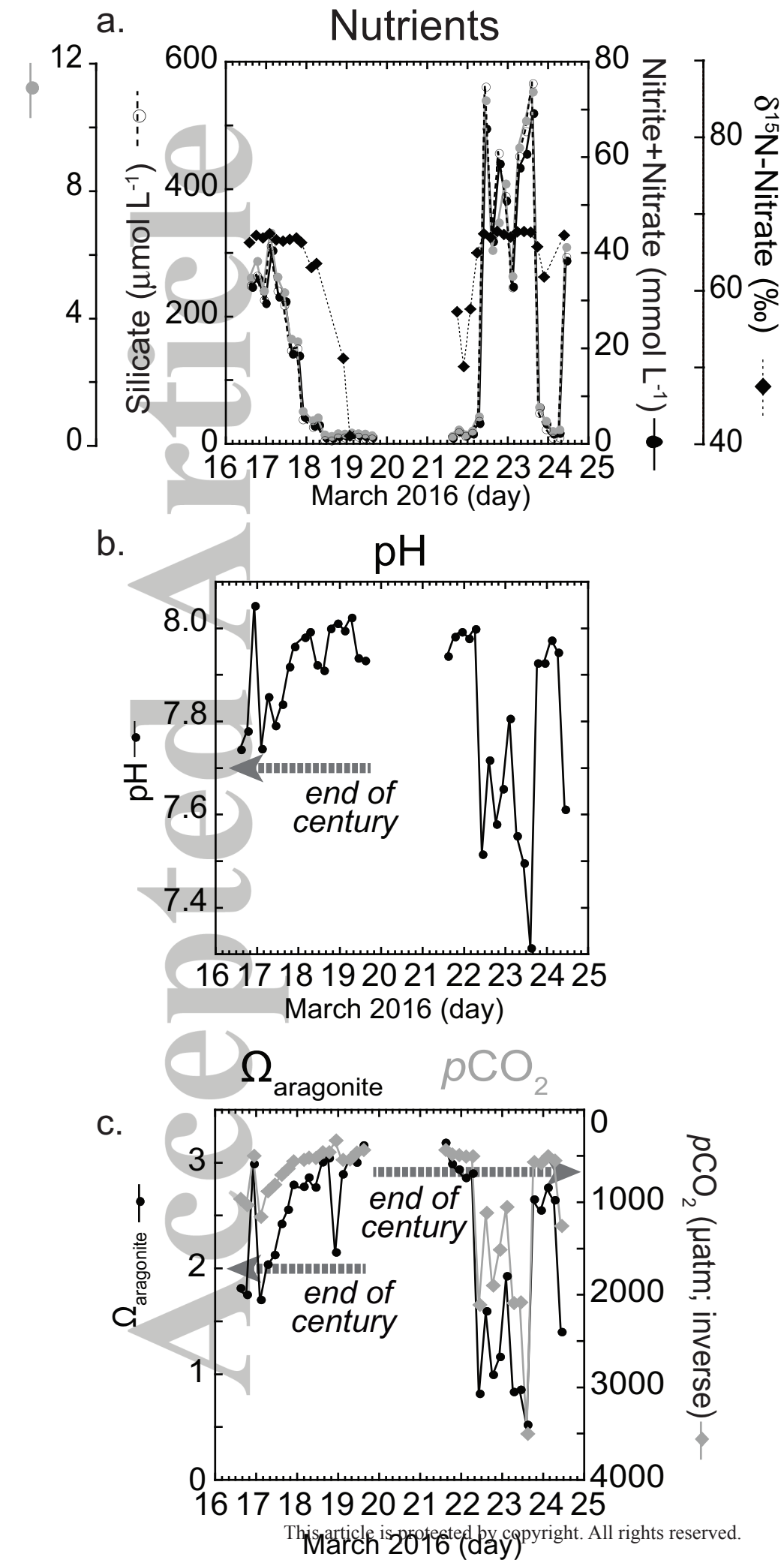

Figure 3.

Figure 3